



ISSN 2314-5609
Nuclear Sciences Scientific Journal
vol. 4, p 103 -114
2015

RADIOACTIVE SHEAR ZONE AT GABAL ATAITER EL-DAHMI, SOUTHWESTERN SINAI, EGYPT: MINERALOGICAL AND GEOCHEMICAL INVESTIGATIONS

OSAMA R. SALLAM

Nuclear Materials Authority, P.O. Box – 530 Maadi, Cairo, Egypt

ABSTRACT

Radiometric survey of Gabal Ataiter El-Dahmi, southwestern Sinai, revealed that, the shear zone exhibit high radioactive anomalies. The altered younger granites samples show high eU and eTh measurements relative to the fresh samples suggesting an addition of eU and eTh during the secondary processes affecting rocks. The data of major and some trace elements of the examined altered younger granites revealed the enrichment in Al_2O_3 , Fe_2O_3 , FeO, MgO, CaO, Na_2O and P_2O_5 , while they shows depletion in SiO_2 , TiO_2 , MnO and K_2O relative to the fresh samples. Enrichment of Al_2O_3 and depletion of SiO_2 could be attributed to sericitization and desilicification respectively during alteration processes. While the process of Na-metasomatism (albitization) leads to enrichment of Na_2O and depletion of K_2O . The enrichments of Fe_2O_3 and MgO are due to the alteration of biotite (chloritization). Trace elements of the examined altered younger granites show enrichment in Rb, Ba, Zr, Y, Nb, Pb and Cu while they reveals depletion in Sr, Zn, Cr and Ni relative to the fresh samples. XRD analysis and ESEM examination of the altered younger granites indicated that, thorite, uranothorite, monazite, xenotime, allanite, zircon and fluorite are the most important radioactive minerals. Pyrolusite, titanite, columbite-tantalite, hematite, kaolinite and calcite are also detected.

INTRODUCTION

Gabal Ataiter El-Dahmi area is located in the southwestern part of Sinai Peninsula east of Abu Zeneima town. The area is bounded by latitudes $28^{\circ} 52' 00''$ and $28^{\circ} 56' 00''$ N and longitudes $33^{\circ} 21' 00''$ and $33^{\circ} 26' 00''$ E (Fig.1). It can be reached via Wadi Sedri leading to Wadi Iqna at the southern part of the study area. Most of the radioactive occurrences in the basement rocks of Egypt are in the granite rocks and their associated pegmatites. They contain accessory minerals such as zircon, monazite, thorite, uranothorite and allanite (Abd El-Naby and saleh, 2003). Sometimes, these rocks undergo varying degrees of alteration, especially along fracture

planes where hydrothermal solutions penetrate these fractures. Changes in geochemistry, mineralogy and texture of the wall rocks along shear zones attract extensive attention of many authors (Pichavant, 1983; Cerny and Ercit, 1985; Burt, 1989; Schwartz 1990; Abdalla et al., 1996; El Afandy et al., 2000). These changes were considered a guide to an ore and as an indicator of the characters of the hydrothermal solution. Many studies were carried out on the radioactive anomalies occurring at the basement rocks around the study area (Hassan 1997, Sherif 1997, El Mowafy et al., 2003, and El Aassy et al., 2004). The main goal of this paper is focused on the mineralogy and geochemistry of altered younger granites of the studied area.

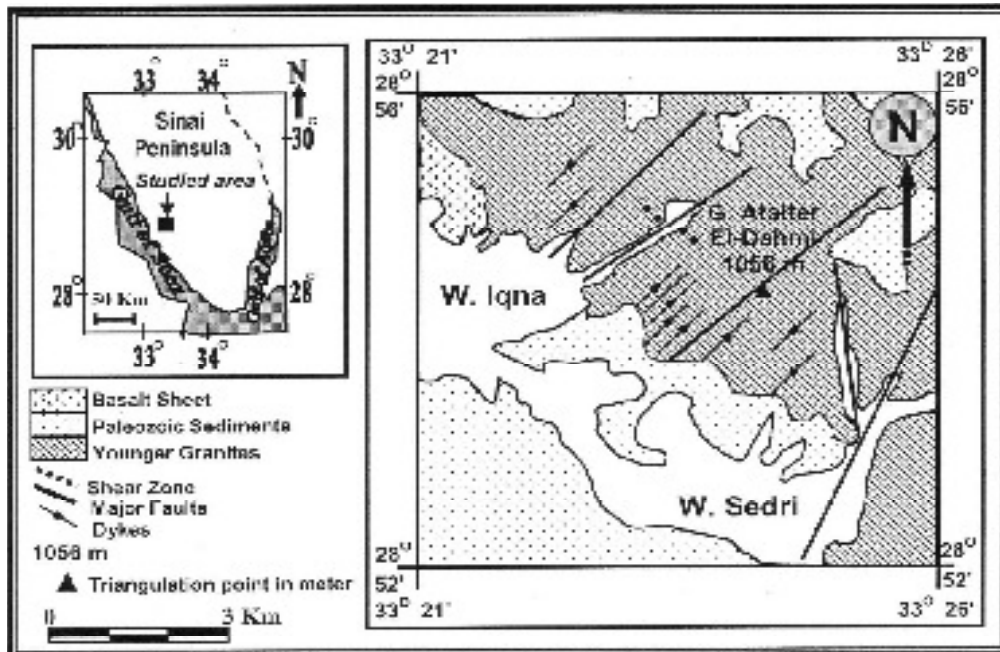


Fig. 1: Geologic map of Gabal Ataiter El-Dahmi area

METHODOLOGY

Ten representative samples of examined rocks were collected (weighting from 3 to 5kg for each sample). In order to determine their mineralogical constituents; the samples were crushed and screened. The fractions having grain size range between 0.074mm and 0.5mm were used. These size fractions were subjected to systematic mineral separation techniques using bromoform (Sp.G. = 2.85) as a heavy liquid and magnetic fractionation using Frantz Isodynamic Magnetic Separator at side slope of 5°, forward slope of 20° and 0.5 A (Flinter, 1959). The obtained heavy mineral fractions were studied under the Binocular microscope as well as X-ray diffraction (XRD) and Environmental Scanning Electron Microscope (XL30-ESEM, Philips) attached with EDAX microanalysis unit developments in high-pressure (low-vacuum). All the samples were chemically analyzed for the major oxides using the wet chemical techniques and the trace elements were measured

using X-ray fluorescence (XRF) and atomic absorption. The radiometric measurements of eU (ppm), eTh (ppm) and K% of the studied fresh and altered younger granites were obtained using a portable differential gamma ray spectrometer model GS-512, serial No. 9805, manufactured by Czech Republic, and the reading were given directly each 30 second. All laboratory works were done in the Central Laboratories of the Nuclear Materials Authority (NMA), Cairo, Egypt.

FIELD GEOLOGY AND PETROGRAPHY

The study area at Gabal Ataiter El-Dahmi is mainly covered by Precambrian monzo and syanogranites and Paleozoic sedimentary rocks. Granites are mainly coarse to medium-grained, buff and pink to reddish pink in color, highly jointed in different directions. They enclose xenoliths of older granites with sharp contacts and different sizes (Fig. 2). The study younger granites are traversed by

shear zone (varies from 15 to 20 m in width and about 750m extension) trending N 45° W - S 45° E with nearly vertical dip (Fig. 3). Pegmatite occurs as pockets (Fig. 4) invading granites in the shear zone, also, iron oxides and quartz veins occur as fractures filling (Fig. 5). The main types of alteration along the shear zone are desilicification, hematitization and kaolinitization (Fig. 6) representing the post-magmatic hydrothermal alterations.

The modal composition of plagioclase (P), K-feldspar (A) and quartz (Q) of the studied granites is listed in Table (1) and the obtained data are plotted on the QAP dia-



Fig.4: Pegmatite pocket invading younger granites in the shear zone



Fig.2: Rounded xenoliths of older granites in monzogranite



Fig.5: Iron oxides and quartz veins occurred as fractures filling in the shear zone



Fig.3: Fractured younger granites along shear zone, looking SE



Fig.6: kaolinitization along fractures in the shear zone

Table 1: Modal composition of the studied granites

Rock Units	Felsic Minerals					Accessory Minerals	Q	A	P
	Qz	k-fel.	Plag.	Mus	Bio				
Monzogranite	37.25	35.31	25.21	0.77	1.31	0.15	34.00	41.00	25.00
	39.47	25.58	29.69	2.82	0.56	1.88	41.00	26.00	33.00
	37.23	25.74	32.10	2.60	1.42	0.91	39.50	26.50	34.00
	47.00	26.06	22.27	2.00	1.93	0.74	43.30	19.30	23.40
	49.52	17.69	27.55	1.69	2.98	0.57	50.30	18.21	31.49
Syenogranite	44.11	41.62	12.76	0.56	0.65	0.30	45.00	42.00	13.00
	36.11	42.45	15.51	1.92	3.21	0.80	42.00	43.00	15.00
	31.99	46.32	18.21	0.99	1.93	0.56	33.00	46.00	21.00
	51.31	39.39	8.31	0.41	0.19	0.23	53.00	39.00	8.00

Qz:quartz; K-fel.: potash feldspar;Plag.: plagioclase;Mus.:muscovite; Bio.:biotite;Hb:hornblende;Q:quartz content;A:potash feldspar content; P: plagioclase content

gram of Streckeisen (1976) (Fig. 7). According to QAP diagram the studied Gabal Ataiter El-Dahmi granites fall within syenogranite and monzogranite fields. Microscopically, the syenogranite is composed of quartz, K-feldspar, plagioclase, biotite and muscovite. Fluorite, zircon, allanite, apatite and opaques are common accessories. The monzogranite is composed mainly of quartz, plagioclase, k-feldspar biotite and hornblende. Sphene, zircon, apatite and opaques are common accessories, whereas chlorite, epidote, kaolinite, sericite are secondary minerals. On the other hand the altered granites at the shear zone are highly sericitized, hematitized, and kaolinized (Fig. 8) resulting from the effect of the hydrothermal solutions. Allanite forms euhedral prismatic crystals associated with biotite and feldspars (Fig. 9). Metamict zircon in which coated by iron oxides is shown along fractured plagioclase and quartz (Figs. 10 a&b respectively).

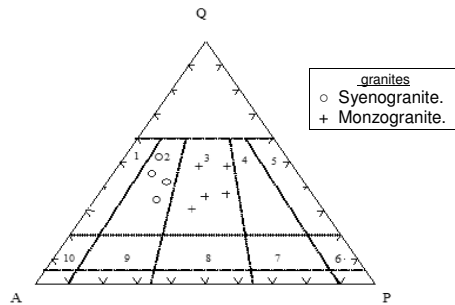


Fig.7: QAP diagram of the studied granites, after Streckeisen (1976) 1 = Alkali feldspar granite, 2 = Syenogranite, 3 = Monzogranite, 4 = Granodiorite, 5 = Tonalite, 6 = Quartz diorite, 7 = Quartz monzodiorite, 8 = Quartz monzonite, 9 = Quartz syenite and 10 = Quartz alkali-feldspar syenite.

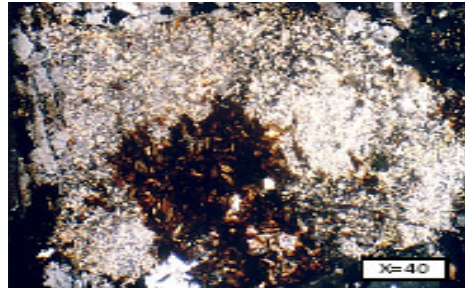


Fig.8: Altered granites in shear zone show Highly sericitized, hematitized, and kaolinized,XPL

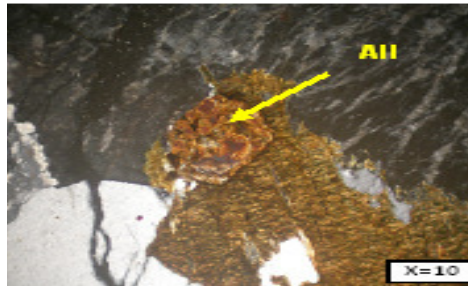


Fig.9: Altered granites in shear zone show Allanite (All) forms euhedral prismatic crystals associated with biotite and feldspars, XPL

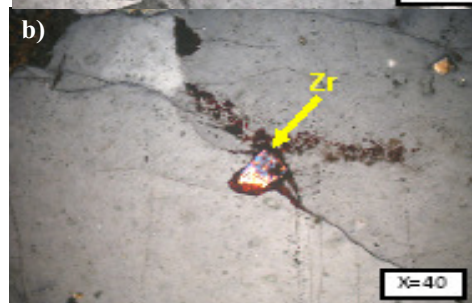


Fig.10: Altered granites in shear zone show metamict zircon (Zr) coated by iron oxides along fractured plagioclase (a) and quartz (b) respectively,XPL

RADIOACTIVITY

Fresh younger granites have wide variation in both eU and eTh contents (Table 2). The eU contents vary between 3.8 and 13.6 ppm with an average 7.4 ppm while eTh contents range between 35.8 and 56.2 ppm with an average 41.07 ppm. The average eTh/eU ratio is 5.8. Normally, thorium is three times as abundant as uranium in rocks (Rogers and Adams, 1969). Stuckless, (1979) recorded that, if the thorium anomalies are accompanied by Th/U ratios greater than 5 uranium loss from the basement rock seems probably.

Altered granites (shear zone) show high value of eU and eTh contents (Table 2), in which eU range between 30.6 and 54.1 ppm with an average 42.49 ppm, while eTh range between 188.4 and 287.3 ppm with an average 243.48 ppm.

Generally, the altered samples from the shear zone show high eU and eTh contents relative to the fresh samples may be due to

the presence of U-Th minerals in the studied samples as well as will be seen later.

The probable origin of the radioactive anomalies recorded in the shear zone could be attributed to the epigenetic concept, in which, the secondary ascending hydrothermal solutions carry out the radioactive minerals to deposit mainly along fractures, faults and shear zones. The presence of fluorite reveals the hydrothermal origin of the mineralization (Sarcia, 1958). The field evidence supports this concept where, the radioactive intensity increases with depth along fractures, faults and shear zones.

In addition to leaching concept; in which, the uranium has been leached from other surrounding rocks, transported by means of circulating water and finally deposited in the shear zone, Attawiya (1983) mentioned that uranium could be released from the granite itself by dissolution of accessory uranium bearing minerals and then re-deposited in shear zones by percolating solution.

Table 2: Radiometric measurements of the studied granites

Altered younger granites (Shear zone)				Fresh younger granites				
eU (ppm)	eTh (ppm)	K %	eTh/eU	eU (ppm)	eTh (ppm)	K %	eTh/eU	
54.1	218.3	8.5	4.04	7.1	51.1	7.0	7.20	
35.4	287.3	9.1	8.12	6.7	38.1	6.8	5.69	
30.6	231.8	8.9	7.58	5.3	43.5	5.7	8.21	
43.2	248.7	6.7	5.76	5.6	38.0	6.8	6.79	
42.8	193.1	6.1	4.51	13.6	38.0	6.1	2.79	
33.4	238.3	9.8	7.13	6.1	37.3	6.6	6.11	
45.0	247.6	7.9	5.50	3.8	37.9	6.3	9.97	
34.9	188.4	8.5	5.40	5.9	40.0	5.9	6.78	
54.1	266.7	7.8	4.93	7.9	38.8	6.2	4.91	
51.4	269.6	7.3	5.25	9.9	56.2	7.1	5.68	
Max.	54.1	287.3	9.8	8.12	6.4	48.1	6.7	7.52
Min.	30.6	188.4	6.1	4.51	6.9	39.6	6.9	5.74
Average	42.49	243.48	8.06	5.52	7.5	39.6	7.2	5.74
				7.0	40.2	6.7	5.74	
				6.7	38.5	5.8	5.75	
				5.1	35.8	6.4	7.02	
				10.2	38.3	7.4	3.75	
				9.9	38.6	5.8	3.90	
				10.3	43.6	5.8	4.24	
				6.0	40.1	8.9	6.38	
Max.				13.6	56.2	8.9	9.97	
Min.				3.8	35.8	5.7	2.79	
Average				7.40	41.07	6.61	5.80	

GEOCHEMISTRY

The geochemical characteristics of the studied altered granite at the shear zone were obtained through the analyses of ten representative samples for their major oxides and some trace elements. The data of major and some trace elements as well as CIPW norms of the examined altered granites are given in Table (3).

A comparison between the average of the obtained data and the average chemical composition obtained by El Mowafy et al., 2003 for the fresh granites in the study area (Table 4) was done to evaluate the geochemical behavior of certain elements in the studied altered granites. It is revealed that, the altered samples show enrichment in Al_2O_3 , Fe_2O_3 , FeO, MgO, CaO,

Na_2O , P_2O_5 and L.O.I, while it shows depletion in SiO_2 , TiO_2 , MnO and K_2O . Depletion of SiO_2 could be attributed to desilicification process. The alteration of feldspars (sericitization) leads to the enrichment of Al_2O_3 . While the process of Na-metasomatism (albitization) leads to enrichment of Na_2O and depletion of K_2O . Enrichment of Fe_2O_3 and MgO are due to the alteration of biotite (chloritization) and hematitization processes.

The high values of the loss of ignition (L.O.I) in the altered samples are due to saturation with intergranular water. On the other hand, the trace elements indicate that, the altered younger granite samples show enrichment in most elements except Sr, Zn, Cr and Ni.

Ab-Qz-Or ternary diagram of Stemprok (1979) and Na_2O - K_2O variation diagram of

Table 3:Chemical analyses and some CIPW norms of the studied altered granites of the studied area

Major oxides	1	2	3	4	5	6	7	8	9	10
SiO ₂	66.11	63.7	65.8	64.7	65.25	63.5	66.3	63.62	63.34	65.41
TiO ₂	0.06	0.2	0.4	0.4	0.3	0.2	0.27	0.36	0.6	0.4
Al ₂ O ₃	15.13	14.95	15.01	14.8	15.14	15.71	15.11	15.7	15.5	15.27
Fe ₂ O ₃	3.2	3.79	3.03	3.04	3.29	4.31	3.09	3.03	3.36	3.15
FeO	1.01	1.6	1.15	1.31	1.33	1.39	1.35	1.39	1.17	1.53
MnO	0.1	0.12	0.18	0.08	0.07	0.07	0.09	0.09	0.11	0.07
MgO	2.0	2.18	2.11	2.71	2.1	2.24	2.13	2.23	2.46	2.79
CaO	2.4	2.01	2.15	2.25	2.37	2.2	2.18	2.75	2.92	2.66
Na ₂ O	4.1	4.77	4.41	4.99	3.94	4.32	4.69	4.81	4.85	3.91
K ₂ O	3.35	4.14	4.1	4.29	4.65	4.22	3.15	4.07	3.94	3.12
P ₂ O ₅	0.20	0.3	0.1	0.2	0.41	0.1	0.3	0.3	0.1	0.3
L.O.I	1.65	1.92	1.5	1.51	1.41	1.73	1.34	1.57	1.62	1.37
Total	99.95	99.98	99.94	99.98	99.98	99.99	100.0	99.92	99.97	99.98
Trace elements (in ppm)										
Rb	327	294	318	311	323	329	309	317	312	323
Sr	19	16	23	20	21	23	21	18	22	18
Ba	765	708	1005	931	1013	884	946	790	982	874
Zr	545	477	648	569	609	665	578	637	622	549
Y	269	235	319	282	303	317	267	289	309	274
Nb	94	82	112	99	106	115	118	77	66	89
Zn	163	159	192	187	182	194	167	184	197	165
Pb	42	47	52	48	54	54	49	51	43	46
V	19	17	25	23	23	25	26	21	19	22
Cr	27	20	20	30	25	29	30	23	27	26
Ni	9	10	8	10	9	8	10	8	9	8
Ga	25	27	33	26	25	28	21	26	25	31
Cu	10	11	15	14	13	11	21	12	22	20
CIPW norms										
Q	22.24	13.84	17.48	11.82	17.16	14.69	20.17	12.31	11.68	21.94
Or	20.18	24.97	24.64	25.77	27.90	25.40	18.88	24.51	23.70	18.71
Ab	35.29	41.11	37.86	42.83	33.78	37.16	40.18	41.38	41.68	33.51
An	10.94	7.25	9.15	5.36	9.99	10.52	9.18	9.35	8.99	11.60

Table 4: Average major and trace element contents of both fresh and altered granites of the studied area

Altered granites (Shear zone)			Fresh granites (El Mowafy et al., 2003)		
Major oxides		Trace elements (ppm)	Major oxides		Trace elements (ppm)
SiO ₂	64.77	Rb 316	SiO ₂	74.27	Rb 248
TiO ₂	0.32	Sr 20	TiO ₂	0.49	Sr 163
Al ₂ O ₃	15.23	Ba 890	Al ₂ O ₃	13.19	Ba 769
Fe ₂ O ₃	3.32	Zr 590	Fe ₂ O ₃	0.96	Zr 228
FeO	1.32	Y 286	FeO	0.56	Y 38
MnO	0.09	Nb 99	MnO	0.14	Nb 28
MgO	2.30	Zn 179	MgO	0.43	Zn 217
CaO	2.39	Pb 49	CaO	0.83	Pb 27
Na ₂ O	4.48	V 22	Na ₂ O	3.40	V 21
K ₂ O	3.90	Cr 26	K ₂ O	4.64	Cr 34
P ₂ O ₅	0.23	Ni 9	P ₂ O ₅	0.09	Ni 23
L.O.I	1.56	Ga 27	L.O.I	0.75	Ga 25
		Cu 15			Cu 11

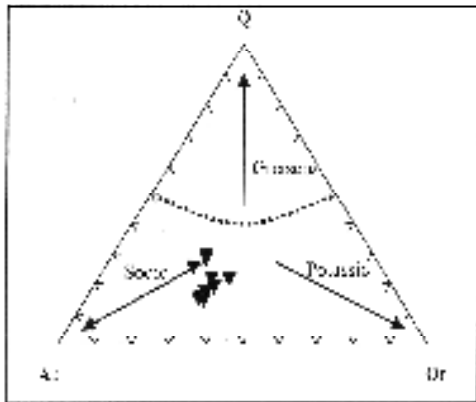


Fig.11: Ab-Q-Or ternary diagram of Stemprok (1979), for the altered granites

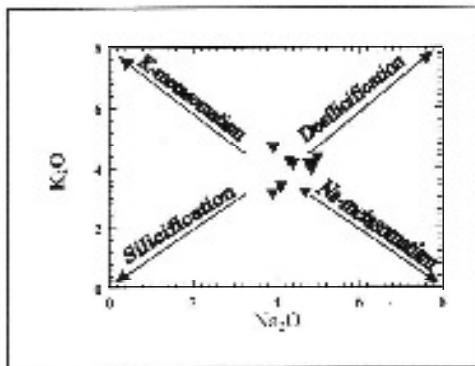


Fig.12: Na₂O-K₂O variation diagram of Cuney et al. (1989), for the altered granites

Cuney et al. (1989) (Fig. 11 & 12 respectively) were used to determine the different types of hydrothermal alterations of the altered granite samples. According to the normative Ab-Qz-Or ternary diagram (Fig. 11) the altered samples characterized by Na-metasomatism during which albitization proceeded through replacement of Na⁺ for K⁺ and Ca²⁺ of the pre-existing feldspars. The Na₂O-K₂O variation diagram (Fig. 12) show albitization followed by desilicification of the examined samples. Al₂O₃ - (Na₂O + K₂O) - (FeO⁺ + MgO + MnO) ternary diagram of Meyer and Hemely (1967) indicated that, the studied samples plotted in the sericite field (Fig. 13).

Formation of albite, sericite, chlorite and hydrothermal leaching of quartz are the most pronounced features of the studied altered granite (albitization, sericitization, chloritization and desilicification). Accordingly, the alteration processes in Gabal Aitaier El-Dahmi area are mostly due to acidic hydrothermal activity changed to alkaline with time.

MINERALOGICAL INVESTIGATIONS

XRD analysis and ESEM examination of the studied altered granites indicated that, the most important radioactive minerals include thorite, uranothorite, monazite, xenotime, allanite, zircon and

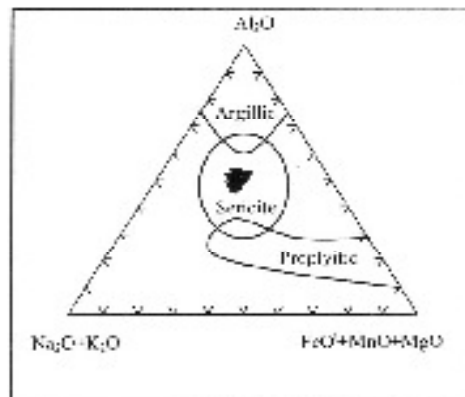


Fig.13: Al₂O₃ - (Na₂O + K₂O)-(FeO⁺+MgO + MnO) ternary diagram of Meyer and Hemely (1967), for the altered granites

fluorite. Pyrolusite, titanite, columbite-tantalite, hematite, kaolinite and calcite are also detected.

Thorite: Th SiO_4

It occurs as brown to black color crystals. Thorite was identified by using the XRD technique (Fig. 14). It contains as much as 10% uranium (Heinrich, 1958).

Uranothorite: $(\text{Th U}) \text{SiO}_2$

Uranothorite occurs as yellow to yellowish brown anhedral to subhedral crystals with rounded corners. It is like thorite but with uranium more than 10%. The ESEM analyses of some uranothorite crystals reveal high values for U-content (17.22 wt %) and normal value of Th and Si-contents (52.93 wt % and 10.95 wt % respectively). Other elements such as Fe, Y, Al, Ca, Mg, Ce, S, V and Cu are present in variable amounts (Fig. 15).

Monazite: $(\text{Ce, La, Th}) \text{PO}_4$

The studied monazite (Fig. 16) grains occur as colorless rounded to subrounded crystals. The ESEM analysis of monazite crystals show that uranium content equals 4.23 wt %, while the thorium content reaches 3.95 wt %, the P-content is 14.64 wt % and the Si-content is 14.21 wt %. Aswathanarayana (1985) and Heinrich (1958) interpret the presence of high silica as may be due to admixed thorite. Also, the analysis proved that monazite occurs as Ce-monazite. Gramaccioli and Segalstad (1978) discussed the possible substitution, which allows tetravalent Th^{4+} and U^{4+} to occupy the trivalent REE position in monazite.

Xenotime: Y PO_4

It was identified by using both the EDAX and XRD techniques (Fig. 17 & 18). It is present as anhedral crystals with yellowish brown to pale yellow color.

Allanite: $(\text{Ca, Ce})_2 (\text{Fe}^{2+}, \text{Fe}^{3+}) \text{Al}_2\text{O} (\text{SiO}_4) (\text{Si}_2\text{O}_7) (\text{OH})$

It is recorded in small amount in the studied samples exhibiting dark brown color (Fig.

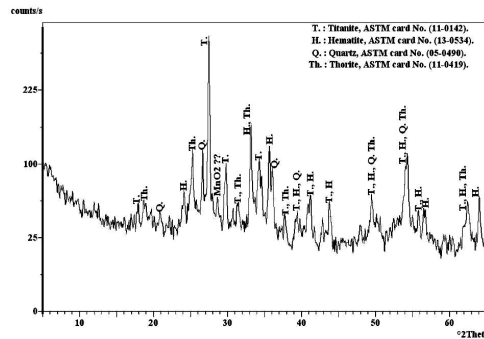


Fig.14: X-ray diffraction patterns of titanite, hematite, quartz and thorite

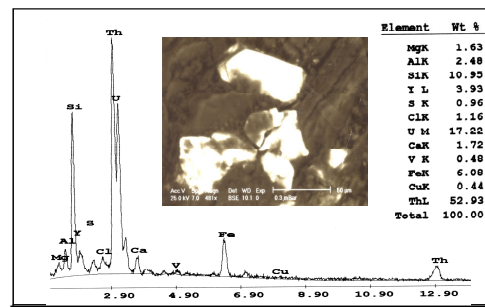


Fig.15: BSE images and EDX charts show Uranothorite

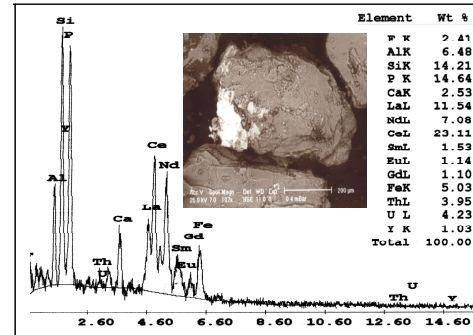


Fig.16: BSE images and EDX charts show Monazite

19). The ESEM and EDAX analysis of allanite reveals that high content of Th (13.46 wt %) and U (11.36 wt %) with appreciable content of REE. In most cases the allanite mineral is uranium and thorium carrier, sometime, altered and inverted to an amorphous substance product by break down of the space lattice by radioactive emanation (Kerr, 1977).

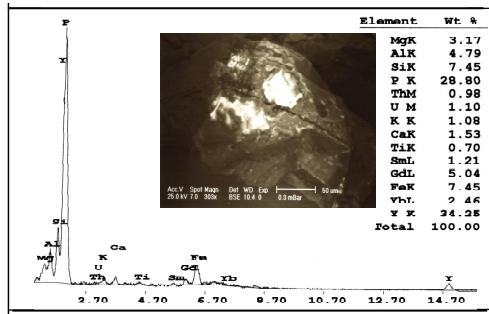


Fig.17:BSE images and EDX charts show xenotime

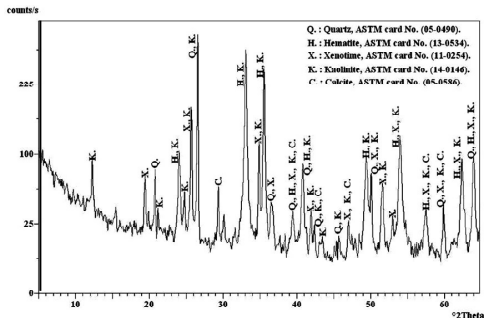


Fig.18:X-ray diffraction patterns showing quartz, hematite,xenotime,kaolinite and calcite

Zircon: $Zr SiO_4$

Zircon (Fig. 20) is the most important radioactive accessory mineral in the granitic rocks (Pagel, 1982). It occurs as euhedral six-sided or eight-sided form with clusters opaque inclusions. It is mainly colourless to pale yellow and associated with iron oxides and fluorite. Thorite and zircon are isomorphous minerals that why a large part of thorium is incorporated in the zircon structure (Rankama and Sahama, 1955).

Fluorite: $Ca F_2$

It occurs as colorless to light-violet in color. Fluorite minerals are possessed vitreous luster and white streak. It is mainly recorded filling cavities and micro-fractures, which reflect their secondary origin as resulting from hydrothermal alteration of younger granites. The studied fluorite shows high content of REE and uranium (Fig.21). Raslan (2009)

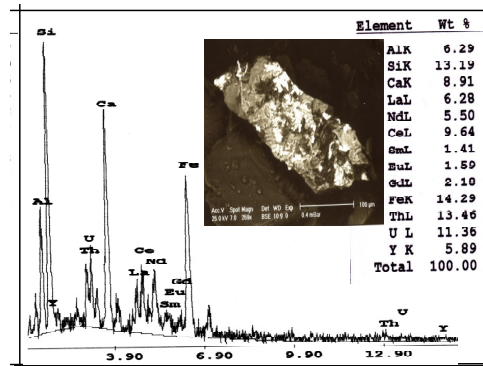


Fig.19: BSE images and EDX charts show allanite

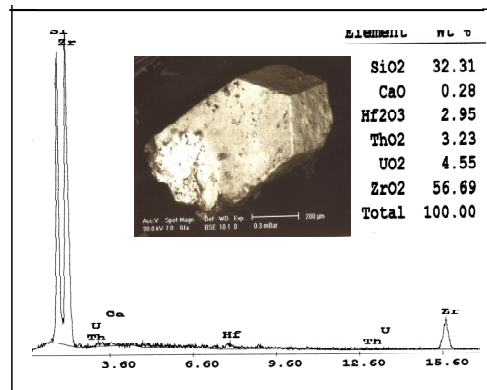


Fig.20: BSE images and EDX charts show zircon

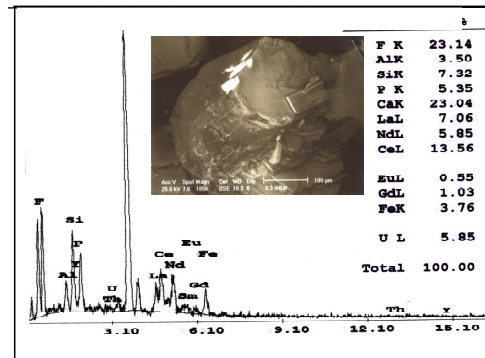


Fig.21: BSE images and EDX charts show fluorite

recorded a highly radioactive fluorite in the jaspoid veins in the sheared granite of El-Missikat pluton.

Pyrolusite: Mn O₂

It is one of the more common manganese minerals. This mineral is recorded in minor amount in the studied samples and has dark steel-gray color (Fig. 22).

Titanite: Ca Ti (SiO₄) O

It was identified by using the EDX-SEM and XRD techniques (Fig. 14&23). It is recorded in the studied samples in appreciable amount. It shows high content of characteristic REE and occurs as pale yellow to brownish yellow with adamantine luster and wedge shaped crystals.

Columbite-Tantalite: (Fe, Mn) (Nb, Ta)₂ O₆

Occur as short prismatic crystals with black to dark black color. EDAX-SEM analysis reveals that, high content of Nb and

Ta (52.45 wt % & 24.12 wt % respectively), while, the uranium content reaches 2.23 wt %, (Fig. 24).

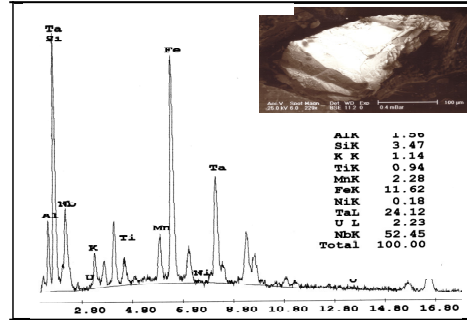


Fig.24: BSE images and EDX charts show columbite-tantalite

CONCLUSIONS

Monzo and syeno-granites in Gabal At-iter El-Dahmi are crosscut by shear zone (varies from 15 to 20 m in width and about 750m length) trending N 45° W – S 45° E with nearly vertical dip. The main types of alteration along the shear zone are hematitization, kaolinitization and desilicification representing the post-magmatic hydrothermal alterations. Radiometric survey indicated that, shear zone exhibit radioactivity higher than the studied un-sheared rocks. The petrographic investigation of the altered granites in the shear zone shows the presence of allanite and metamict zircon. Fresh granites have wide variation in both eU and eTh contents. The eU contents vary between 3.8 and 13.6 ppm with an average 7.4 ppm while eTh contents range between 35.8 and 56.2 ppm with an average 41.07 ppm. The average eTh/eU ratios is 5.8. Altered younger granites (shear zone) show high value of eU and eTh contents, in which eU contents range between 30.6 and 54.1 ppm with an average 42.49 ppm, while eTh contents range between 188.4 and 287.3 ppm with an average 243.48 ppm. Generally, the altered samples show high eU and eTh contents relative to the fresh samples suggesting an addition of both U and Th during the secondary processes affecting

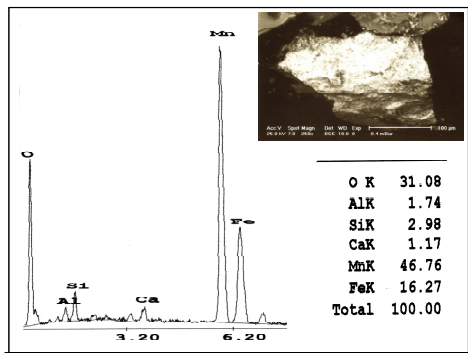


Fig.22: BSE images and EDX charts show Pyrolusite

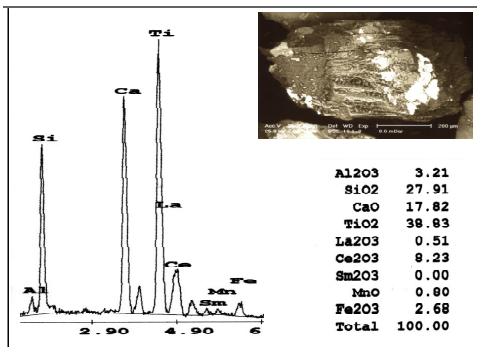


Fig. 23: BSE images and EDX charts show titanite

rocks. The probable origin of the radioactive anomalies recorded in the shear zone could be attributed to the epigenetic concept, in which, the secondary ascending hydrothermal solutions carry out the radioactive elements to deposit mainly along fractures, faults and shear zones. The data of major elements of the examined altered granites show enrichment in Al_2O_3 , Fe_2O_3 , FeO , MgO , CaO , Na_2O , P_2O_5 and $L.O.I$, while it shows depletion in SiO_2 , TiO_2 , MnO and K_2O relative to the fresh samples. Enrichment of Al_2O_3 and depletion of SiO_2 could be attributed to sericitization and desilicification respectively during alteration processes. While, the enrichment of Na_2O and depletion of K_2O are due to the process of Nametasomatism (albitization). The altered granite samples show enrichment in most trace elements except Sr, Zn, Cr and Ni relative to the fresh samples. XRD analysis and ESEM examination of the altered younger granites indicated that, uranothorite, thorite, monazite, xenotime, allanite, zircon and fluorite are the most important radioactive minerals. Pyrolusite, titanite and columbite-tantalite are also identified.

REFERENCES

- Abdalla, H. M.; Ishihara, S.; Matsueda, H., and Abdel-Monem, A.A., 1996. On the albite-enrichment granitoids at Um Ara area, Southeastern Desert, Egypt; I. Geochemical, ore potentiality and fluid inclusions studies [J]. *J. Geochemical exploration*, 57, 127-138.
- Abd El-Naby, H.H., and Saleh, G.M., 2003. Radioelement distributions in the Proterozoic granites and associated pegmatites of Gabal El Fereyid area, south Eastern Desert, Egypt [J]. *Applied radiation and Isotope*, 59, 289-299.
- Aswathanarayan, U., 1985. Principles of Nuclear Geology. Sauger Univ., India, 88-90.
- Attawiya, M. Y., 1983. Mineralogical study of El-Erediya-1 uranium occurrence, Eastern Desert, Egypt. *Arab. J. Nucl. Sci. Tech.*, 16, 221-234.
- Burt, D.M., 1989. Compositional phase relations among rare earth elements. In: *Geochemistry and Mineralogy of Rare Earth Elements* (Lipin B.R. and McKay G.A., Eds.). *J. Mineral. Soc. Amer.*, 21, 257-307.
- Cerny, P., and Ercit, T.c., 1985. Some recent advances in the mineralogy and geochemistry of Nb and Ta in rare-metal granitic pegmatites [J]. *Bull. Mineral.* 10, 499-532.
- Cuney, M.; Leorty, J.; Valdiviexo, P.A.; Daziano, C.; Gamba, M.; Zarco, J.; Morello, O.; Ninci, C., and Molina, P., 1989. Geochemistry of uranium mineralized Achala Granitic Complex, Argentina; Comparison with Hercynian peraluminous leucogranites of Western Europe. *Metallogensis of uranium Deposits* [M]. IAEA-Tc_452/6, Vienna. 211-232.
- El Aassy, I.E.; El Metwally, A.A.; Sherif, H.M.; Abu Bakr, M.A., and Bishr, A.H., 2004. Uranium mineralizations of Wadi Um Hamad younger granites, southwestern Sinai, Egypt. 6th Inter. Conf. Geochem., Alex. Univ., Egypt, 413-427.
- El Afandy, A.H.; Abdalla, H.A., and Ammar, F., 2000. Geochemistry and radioactive potentiality of Um Naggat Apogranite, Central Eastern Desert, Egypt [J]. *Res. Geol.*, 50, 39-51.
- El Mowafy, A.A.; Hilmy, M.E.; El Aassy, I.E., and Sallam, O.R., 2003. Geological, geochemical and radiometrical studies of the basement rocks around Um Bogma area southwestern Sinai, Egypt. *Egypt. J. Geol.*, 47/1, 215-238.
- Flinter, B.H., 1959. A magnetic separation of some alluvial minerals in Malaya. *Amer. Mineralogist*, 44, No. 7-8, 738-751.
- Gramaccioli, C. M., and Segalstad, T. V., 1978. U- and Th-rich monazite from south-alpine pegmatite at Piona. Italy: *Am. Miner.*, 63, 757-761.
- Hassan, I. H., 1997. Geology and radioactivity of the basement rocks of Wadi El-Shallal area, southwestern Sinai, Egypt. M.Sc. Thesis, Fac. Sci., Ain Shams Univ., 156 p.
- Heinrich, E. W., 1958. Mineralogy and geology

- of radioactive raw materials. Mc-Graw Hill Book Company, Inc. New York, Toronto, London. 654 p.
- Kerr, P.f., 1977. Optical Mineralogy. 4th Ed., Mc-Graw-Hill Book Inc., 492 p.
- Meyer, C.H., and Hemely, T. T., 1967. Wall-Rock alteration. In: geochemistry of hydrothermal deposits (Barnes H.I.,Ed.) [M]. Holt, Rinehart Winston, New York, 166-235.
- Pagel, M., 1982. The mineralogy and geochemistry of uranium, thorium and rare elements in two radioactive granites of Vosges France. Min. Mag., 46 (339), 149-161.
- Pichavant, M., 1983. (Na, K) Exchange between alkali feldspars and aqueous solutions containing borate and fluoride anions, experimental results at P=1 K bar [Z]. 3rd NATO Adv. Stud. Inst., Feldspars and feldspathoids, Rennes. 102 p.
- Rankama, K., and Sahama, T. G., 1955. Geochemistry. Chicago Univ. Press, Chicago, 37 p.
- Raslan, M.F., 2009. Mineralogical and geochemical characteristics of uranium-rich fluorite in El-Missikat mineralized granite, Central Eastern DESERT, Egypt. Geologija, 5212, 213-220.
- Rogers, J. J., and Adams, J. A., 1969. Uranium and thorium, in: Handbook of geochemistry (Wedepohl, K. H.,Ed.). Berlin, Springer-Verlag, 11-3, 92-B-1 to 92-0-8 and 90-Bb-1 to 90-00-5.
- Sarcia, J.A., 1958. The uraniferous province of northern Limousin and its three principal deposits, Peaceful Uses of atomic Energy, IAEA. Conf., 2.
- Schwartz, M.O., 1990. Geochemical criteria for distinguishing magnetic and metasomatic albite-enrichment in granitoids: Examples from the Ta-Ti granite [Yichum (China)] and the Sn-W deposit Tikus (Indonesia) [J]. Mineral. Deposita, 27, 101-108.
- Sherif, H. M. Y., 1997. Geology and uranium potentiality of Wadi Seih area, southwestern Sinai, Egypt. Ph.D. Thesis, Fac.Sci., Cairo Univ., 229 p.
- Stempork, M., 1979. Mineralized granites and their origin [J]. Episodes, 3, 20-24.
- Streckeisen, A., 1976. To each plutonic rocks its proper name. Earth Sci. Rev., 12, 1-33.
- Stuckless, J. S., 1979. Uranium and thorium concentrations in Precambrian granites as indicators of a uranium province in central Wyoming. Contrib. Geology. Univ., Wyo., 17/2, 173-178.

نطاق قص مشع بجبل أظعير الداهمي جنوب غرب سيناء-مصر:

دراسات معدنية و جيوكيميائية

أسامه رياض محمد سلام

يتناول البحث دراسة نطاق قص مشع بجبل أظعير الداهمي من خلال الدراسات الحقلية، البتروجرافية، الإشعاعية، الكيميائية والمعدنية. أوضحت الدراسة الحقلية والبتروجرافية لجبل أظعير الداهمي انه يتكون من صخور الجرانيت الحديث وقد قطع بالبليجماتايت و نطاق القص. من دراسة توزيع النشاط الإشعاعي في صخور الجرانيت الحديث و صخور الجرانيت الحديث المكونة لنطاق القص لوحظ وجود نشاط اشعاعي داخل نطاق القص. كذلك وجدت شاذات اشعاعية بنطاق القص يصل متوسط محتوى اليورانيوم بها ٤٩, ٤٢ جزء في المليون و متوسط محتوى الثوريوم ٤٨, ٤٣ جزء في المليون. الدراسة الكيميائية اظهرت ان صخور الجرانيت الحديث المكونة لنطاق القص غنية بعناصر أكاسيد الالومنيوم، الحديد، الماغنسيوم، الكالسيوم و الصوديوم و كذلك غنية بالعديد من العناصر الشحيحة مقارنة بصخور الجرانيت الحديث خارج نطاق القص و ذلك لتأثر نطاق القص بالعديد من عمليات التعرية و المحاليل الحارة التي تمر من خلاله. الدراسة المعدنية لصخور الجرانيت الحديث المكونة لنطاق القص أوضحت وجود المعادن المشعة التالية: ثوراييت، يورانوثوراييت، مونايزيت، زينونيم، الأنايت، زيركون و فلوراييت. كذلك وجود معادن البيرولوسايت، تيتاناييت، كلومبايت-تانتالييت، هيماتاييت، كاولين و كالساييت.